

Sulfur-Cycling in Methane-Rich Ecosystems:  
Uncovering Microbial Processes and Novel  
Niches

Thesis by  
Abigail Green Saxena

In Partial Fulfillment of the Requirements for the degree  
of  
Doctor of Philosophy



CALIFORNIA INSTITUTE OF TECHNOLOGY  
Pasadena, California  
2013  
(Defended 20 May 2013)



*Chapter 3\**

**\*This chapter, written by Abigail Green Saxena, is being combined with another dataset to be submitted to a peer-reviewed journal.**

**Effects of the sulfate reduction-inhibitor molybdate on anaerobic methane-oxidizing community metabolism, ANME/bacterial aggregate composition and cell growth**

*A. Green-Saxena<sup>1</sup> and V.J. Orphan<sup>2</sup>*

Divisions of <sup>1</sup>Biology and <sup>2</sup>Geological and Planetary Sciences, and <sup>3</sup>Global Environmental Center, California Institute of Technology, 1200 East California Boulevard, Pasadena, CA 91125

## ABSTRACT

Here we show a detailed study in which AOM sediment collected from Hydrate Ridge was amended with sodium molybdate and  $^{15}\text{N}$ -labeled ammonium under a methane headspace and incubated for 13 months. Sulfide production along with sulfate depletion was monitored and supported the complete inhibition of sulfate reduction throughout the incubations. Counts of aggregates hybridized with ANME- and bacterial-specific mono-labeled oligonucleotide probes show that with time, there was a shift in the aggregate composition favoring ANME-only aggregates in inhibited incubations only, suggesting the bacterial partner may be decaying rather quickly in the absence of its primary ability to harvest energy, while ANME cells persist. In order to determine if the remaining primarily ANME-only aggregates were still growing we used fluorescence *in situ* hybridization coupled to nano-scale secondary ion mass spectrometry (FISH-NanoSIMS) to quantify  $^{15}\text{N}$ -ammonium incorporations in the aggregates after 7 months. In non-inhibited controls  $^{15}\text{N}$ -ammonium incorporation (avg. 5.6 atom%) was well above that of natural abundance (0.36 atom%). However, in the inhibited treatment, aggregates showed an average of 0.58 atom%  $^{15}\text{N}$  incorporation, which is not above the background value for potential abiotic adsorption of  $^{15}\text{N}$ -ammonium (0.60 atom%), suggesting little to no incorporation occurred. These data suggest that while the SRB decay and the ANME persist, the ANME are not able to synthesize new proteins and thus are not able to grow when sulfate reduction is inhibited.

## INTRODUCTION

The anaerobic oxidation of methane (AOM) is responsible for recycling up to 80% of the oceanic methane production (Reeburgh, 2007). This crucial biogeochemical process serves as a major sink for methane, a greenhouse gas with heat trapping capabilities up to 20 times stronger than CO<sub>2</sub> (Schiermeier, 2006). Syntrophic aggregates of anaerobic methane-oxidizing archaea (ANME) and sulfate-reducing bacteria (SRB) appear to carry out the anaerobic oxidation of methane (Orphan et al., 2001a). In the following putative pathway, sulfate serves as the electron acceptor for methane (Boetius et al., 2000; Iverson and Jorgensen, 1985):  $\text{CH}_4 + \text{SO}_4^{2-} \rightarrow \text{HCO}_3^- + \text{HS}^- + \text{H}_2\text{O}$ . However, to date, neither ANME nor SRB involved in this reaction have been grown in pure culture, and thus the pathway for AOM, including the method for electron transfer, remains unclear (Knittel and Boetius, 2009). Indeed, Milucka and colleagues (2012) recently proposed a new pathway in which ANME-2 is capable of both the anaerobic oxidation of methane and reduction of sulfate to disulfide (or other S<sub>0</sub> compounds), which is then scavenged by the SRB and disproportionated to sulfide and sulfate.

As sulfate-reducing bacteria were initially implicated as an agent responsible for AOM (Reeburgh, 1976), multiple studies have used sulfate reduction inhibitors such as molybdate or tungstate to validate and study dynamics of AOM (Alperin and Reeburgh, 1985; Hansen et al 1998; Iversen et al., 1987; Nauhaus et al., 2005; Orcutt et al., 2008). Molybdate is a commonly used sulfate reduction inhibitor as it serves as a structural

analogue to sulfate (Reuveny, 1977) and several studies have demonstrated that it successfully inhibits the SRB community in a mixed enrichment culture including non-SRB members (Lovely et al., 1982; Compeau and Bartha, 1985). While earlier studies investigating AOM found little to no inhibition of methane oxidation by sulfate-reduction inhibitors (Alperin and Reeburgh, 1985; Hansen et al 1998; Iversen et al., 1987), Hoehler et al. (1994) point out that conditions of such studies may have led to an increase in methanogenesis, confounding the results. More recent studies from different habitats report near to complete AOM inhibition (Nauhaus et al., 2005; Orcutt et al., 2008).

Due to the difficulties of getting the ANME/SRB consortia into pure culture, prior sulfate-reduction inhibition studies are based on bulk geochemical measurements in which they inhibit sulfate reduction in an entire community and measure the AOM of that community (Alperin and Reeburgh, 1985; Hansen et al 1998; Iversen et al., 1987; Nauhaus et al., 2005; Orcutt et al., 2008). This allows us to see the effect of sulfate reduction inhibition on AOM as a whole it does not show what is happening to the AOM consortia on a cellular level, knowledge which could shed light on the dynamics of this symbiosis. Whether either partner in the symbiosis is able to persist, metabolize and grow in the presence of sulfate-reducing inhibitors remains unclear.

Tracking the effects of sulfate-reducing inhibitors on aggregate abundance and composition can be accomplished via fluorescence *in situ* hybridization (FISH) which can then be coupled to nano-scale secondary ion mass spectrometry (NanoSIMS) in order to measure growth in consortia incubated with  $^{15}\text{N}$ -labeled ammonium (Orphan et al., 2009). FISH-NanoSIMS allows the coupling of function with identity through the measurement of  $^{15}\text{N}$  incorporation in individual cells or aggregates whose phylogenetic identity is

determined via FISH. Here we use a combination of geochemical studies, FISH, and FISH-nanoSIMS to study the effects of a sulfate reduction inhibitor on the metabolic processes and growth of the ANME and bacterial cells involved in AOM.

## **METHODS**

### **Site Selection, Sampling and Processing:**

Push core samples were collected in August 2010 (AT 15-68) from active methane seeps in Hydrate Ridge (Boetius and Seuss 2004) off the coast of Oregon using manned submersible Alvin. Push core PC9 was collected through a microbial mat (Hydrate Ridge South, AD4629, 44°N 34.09 125°W 9.14, 774 m water depth). Microcosm experiments from the top 0-3 cm of PC9 sediment were set up shipboard. Sediments were mixed approximately 1:3 with filtered seawater (sparged with argon) and aliquotted into 40 ml glass bottles (with butyl stoppers) with a 20 ml methane headspace (overpressured to 30 psi). The sediment slurries were amended with 0 or 2 mM <sup>15</sup>N-ammonium and 0 or 25 mM sodium molybdate and incubated anaerobically at 4-8 °C. Killed controls were amended with 2 mM <sup>15</sup>N-ammonium and treated with formaldehyde (final concentration of 3.7%). Sediment samples were taken anaerobically via syringe at 0, 1, 3 and 7 months.

### **Fluorescence *in situ* Hybridization (FISH) and aggregate counts:**

Sediment samples were fixed in 2% paraformaldehyde for approximately 1 hour at room temperature, washed twice with phosphate-buffered saline (PBS; Pernthaler et al., 2008), once with 1:1 PBS: ethanol, resuspended in 100% ethanol and stored at -20°C. For FISH analyses, 150 µl fixed sediment was brought to 0.9 ml in a TE (10 mM Tris-HCl and 1 mM

EDTA (pH 9.0)), 0.01 M pyrophosphate solution, heated in a histological microwave oven (Microwave Research and Applications, Carol Stream, IL) for 3 minutes at 60°C. Samples were then cooled to room temperature and sonicated on ice for 3 10 second bursts with a Vibra Cell sonicating wand (Sonics and Materials, Danbury, CT) at an amplitude setting of 3.0. Percoll (900 µl) was then added to the bottom of the 2 ml tubes, which were then centrifuged at 14000 rpm for 20 minutes at 4°C. The supernatant was filtered onto a 3.0 µm pore-sized polycarbonate filter (Millipore, Billerica, MA). A Cy3-labeled oligonucleotide probe targeting anaerobic methane-oxidizing archaeal clade ANME-2 (Eel\_MS\_932; Boetius et al., 2000) and a FITC-labeled general bacterial probe (EUB338 mix; Amann et al., 1995) were then used in a FISH reaction following the protocol outlined in Orphan et al (2001). Micrograph images were taken with a Deltavision RT microscope system (Applied Precision, Issaquah, WA). ANME/EUB and ANME-only aggregates were counted from a total of 50 aggregate-containing fields per sample. Relative numbers of ANME-only aggregates are expressed as percent ANME-only of total hybridized aggregates.

### **Fluorescence *in situ* Hybridization Nanoscale Secondary Ion Mass Spectrometry (FISH-NanoSIMS):**

Five aggregates from an ammonium- and sodium molybdate-amended incubation (2 mM <sup>15</sup>N-ammonium, 25 mM sodium molybdate, sampled at 7 months), and two aggregates from an ammonium-amended (2 mM <sup>15</sup>N-ammonium, sampled at 7 months) incubation were examined; all incubations were inoculated with methane seep sediment slurries from a push core collected through a microbial mat in Hydrate Ridge (PC-9,

AD4629, AT 15-68).

Fixed and washed sediment samples (150  $\mu$ l) for FISH analysis were treated as described above and applied to a Percoll density gradient as described in Orphan et al (2002). All samples were deposited onto custom cut indium tin oxide (ITO) coated glass and hybridized with Cy3- and FITC-labeled oligonucleotide probes Eel\_MS\_932 (Boetius et al., 2000) and EUB338 (Amann et al., 1995) and mapped for nanoSIMS analysis (Orphan et al., 2002; Dekas and Orphan, 2011). Clostridia spores (with known  $\delta^{13}\text{C}$  and  $\delta^{15}\text{N}$ ) were spotted onto a blank section of a separate ITO coated glass square and used as standards during the analysis. Samples were analyzed using a CAMECA NanoSIMS 50L housed at Caltech, using a mass resolving power approximately 5,000.

A primary  $\text{Cs}^+$  ion beam (0.5 to 1.5 pA) was used to raster over target cells, with a raster size ranging from 10 to 30  $\mu\text{m}$ . Secondary ion images were collected at 256 x 256 pixel resolution with a dwell time of 3,000 to 8,000 ct/pixel over a period of 5 to 12 hours, resulting in 54 to 129 cycles, depending on target size. Due to time constraints, aggregates were not sampled through their entire Z planes. Clostridia spores were measured in ion image mode using the same range in ion beam current as a standard to ensure there were no matrix effects in the analysis. Several masses were collected in parallel including:  $^{12}\text{C}^{14}\text{N}^-$ , and  $^{12}\text{C}^{15}\text{N}^-$  using electron multiplier detectors. Resulting ion images were processed using the L'Image software (developed by L. Nittler, Carnegie Institution of Washington, Washington D.C.). The reported isotope ratio for each aggregate was extracted from the image by identifying a region of interest (ROI) – the aggregate – within each image. The aggregate edge was automatically defined in L'Image by setting a lower threshold of 5% of the maximum value of  $^{12}\text{C}^{15}\text{N}/^{12}\text{C}^{14}\text{N}$  counts within a given cycle. If this automatic ROI

definition included non-aggregate elements from the surrounding area, the portion of the ROI that only contained the aggregate was traced manually and subsequently used as the final ROI. The ratio from the cycle with the highest  $^{12}\text{C}^{15}\text{N}/^{12}\text{C}^{14}\text{N}$  was then collected from each aggregate. The  $^{12}\text{C}^{15}\text{N}/^{12}\text{C}^{14}\text{N}$  ratio is hereafter referred to as the  $^{15}\text{N}/^{14}\text{N}$  ratio.

### **Geochemistry:**

In order to analyze sulfide concentrations in the microcosms at each time point, subsamples of the aqueous phase of incubated sediment slurries (the initial time point was taken from an aliquot of the original un-amended sediment slurry) were filtered via a 0.2  $\mu\text{m}$  filter and combined with 1 M zinc acetate at a 1:1 ratio. Sulfide concentration was then determined using a colorimetric Cline assay (Cline, 1969) measured on a 96-well format TECAN Sunrise spectrophotometer (TECAN, Männedorf, Switzerland).

In order to determine sulfate concentrations, subsamples of the aqueous phase of incubated sediment slurries were filtered via a 0.2  $\mu\text{m}$  filter and frozen at  $-20^{\circ}\text{C}$  until analysis. Parallel ion chromatography systems operated simultaneously (Dionex DX-500, Environmental Analysis Center, Caltech) were used to measure ammonium, nitrate, nitrite and sulfate in the porewater samples. A single autosampler loaded both systems' sample loops serially. The 10  $\mu\text{l}$  sample loop on the anion IC system was loaded first, followed by a 5  $\mu\text{l}$  sample loop on the cation IC system. Temperatures of the columns and detectors were not controlled.

Nitrite, nitrate and sulfate were resolved from other anionic components in the sample using a Dionex AS-19 separator (4x250 mm) column protected by an AG-19 guard (\*4x50 mm). A hydroxide gradient was produced using a potassium hydroxide eluent

generator cartridge and pumped at 1 mL per minute. The gradient began with a 10 mM hold for 5 minutes, increased linearly to 48.5 mM at 27 minutes and finally to 50 mM at 41 minutes. 10 minutes were allowed between analyses to return the column to initial conditions. Nitrite and nitrate were determined for UV absorption at 214 nm using a Dionex AD25 Absorbance detector downstream from the conductivity detection system. Suppressed conductivity detection using a Dionex ASRS-300 4 mm suppressor operated in eluent recycle mode with an applied current of 100 mA was applied to detect all other anions, including redundant measurement of nitrite and nitrate. A carbonate removal device (Dionex CRD 200 4 mm) was installed between the suppressor eluent out and the conductivity detector eluent in ports.

Ammonium was resolved from other cationic components using a Dionex CS-16 separator column (5x250 mm) protected by a CG-16 guard column (5x50). A methylsulfonate gradient was produced using a methylsulfonic acid based eluent generated cartridge and pumped at 1 mL per minute. The gradient began with a 10 mM methylsulfonate hold for 5 minutes, then increased to 20 mM at 20 minutes following a non-linear curve (Chromleon curve 7, concave up), increased further to 40 mM at 41 minutes following a non-linear curve (Chromleon curve 1, concave down). 10 minutes were allowed between analyses to return the column to initial conditions. Suppressed conductivity detection using a Dionex CSRS-300 4 mm suppressor operated in eluent recycle mode with an applied current of 100 mA.

Standard curves were generated for each species. For nitrate, nitrite, and sulfate, standard measurements were fitted to a linear curve; for ammonium, standard measurements were fitted to a quadratic curve. Standard ranges were 10  $\mu$ M to 2 mM

(nitrate, nitrite) and 500  $\mu\text{M}$  to 32 mM (sulfate). Standard deviation of repeated injections of a standard (250  $\mu\text{M}$  nitrate and nitrite, 8000  $\mu\text{M}$  sulfate) throughout the analysis were 4.2  $\mu\text{M}$  (nitrate), 5.8  $\mu\text{M}$  (nitrate) and 113  $\mu\text{M}$  (sulfate).

## RESULTS AND DISCUSSION

### Geochemistry

Sulfide production was measured as a proxy for sulfate reduction in four sets of duplicate incubations: Blank (no amendments), non-inhibited control (2 mM  $^{15}\text{N}$ -ammonium added), a killed control (2 mM  $^{15}\text{N}$ -ammonium; treated with formaldehyde at initial time point) and an incubation in which sulfate reduction was inhibited (25 mM sodium molybdate, 2 mM  $^{15}\text{N}$ -ammonium). The killed control and inhibited incubations exhibited little to no sulfide production over the course of 13 months, suggesting no sulfate reduction occurred in these samples (Figure 1). The small increase in sulfide between the 0 and 1 month time points (< 1 mM increase) may be an artifact of sampling; the initial time point was taken from an aliquot of the original un-amended sediment slurry and may thus vary slightly from the sulfide levels in the respective incubation bottles listed above. The blank and non-inhibited control incubations showed a large increase in sulfide (> 14 mM) from the 0 to 1 month time point. Interestingly, all of these high sulfide accumulation incubations had instances of sulfide loss at various point between the 1 and 13 month time points. These data suggest that either 1. sampling error occurred and sulfide was lost due to abiotic oxidation or 2. some component of the incubation was able to oxidize sulfide *in situ*. The latter may result from the likely presence of sulfur-oxidizing bacteria in the incubations, the sediment for which was collected from the top 3 cm horizons of a push core collected through a sulfur-

oxidizing microbial mat. Several species of sulfur-oxidizers can store nitrate intracellularly for use as a terminal electron acceptor in the sulfide oxidation reaction and thus would be viable in these anaerobic incubations (Preisler et al., 2007). This metabolic reaction produces ammonium, which was seen to accumulate in the amendment-free “blank” incubations (the addition of 2 mM ammonium results in concentrations above the detection limit in other incubations) in which ammonium levels increase from 559 and 755  $\mu\text{M}$  ammonium at 1 month to 1463 and 1580  $\mu\text{M}$  at 13 months in incubations Blank A and Blank B, respectively.

Sulfate depletion was also measured in three sets of the same duplicate incubations: Blank (no amendments), non-inhibited control (2 mM  $^{15}\text{N}$ -ammonium added) and an incubation in which sulfate reduction was inhibited (25 mM sodium molybdate, 2 mM  $^{15}\text{N}$ -ammonium). The inhibited incubations show a near constant concentration of approximately 24 mM sulfate from the 1 to 13 month time points, suggesting no sulfate reduction occurred. Blank and non-inhibited control incubations however show a depletion of sulfate below that of 0.8 mM after 13 months, suggesting the majority of the sulfate had been reduced.

### **Change in aggregate abundance and composition over time**

As prior studies have estimated a doubling time of 3 to 7 months for ANME SRB aggregates (Orphan et al., 2009; Nauhaus et al., 2007), we conducted aggregate counts over a period of 7 months (sampling at 0, 1, 3 and 7 months) in the control and inhibited incubations. Total aggregates counted (from 50 aggregate-containing fields per time point) in the control incubation increased with time from 438 at the initial time point to 705 after 7 months,

suggesting growth. However, total aggregates counted in the inhibited incubation were much lower at 7 months (150) than at the initial time point (396). The percent of ANME-only aggregates (out of total ANME-containing aggregates) was initially low in both incubations (10% and 11% in control and inhibited incubations, respectively). Aggregate composition in the control sample showed a relatively slight shift towards ANME-only aggregates at 1 month (23%), which decreased at 3 (18%) and 7 (16%) months (Figure 2). The inhibited incubation revealed a more dramatic and continual shift towards ANME-only aggregates over time, with ANME-only aggregates comprising 83% of total hybridized aggregates at the 7 month time point. Whether the ANME-only aggregates were comprised of new growth or the previously existing ANME/bacterial aggregates in which the SRB cells decayed was unclear based on these data alone. If the ANME-only aggregates observed in the later time points were once ANME/bacterial aggregates it is interesting that the bacterial and not the ANME cells decayed. This would suggest that the bacterial cells do not survive when sulfate-reduction is inhibited whereas the ANME cells are at least able to persist under these conditions. NanoSIMS studies were subsequently done in order to determine if cells in the ANME-only aggregates were actively growing.

### **FISH-NanoSIMS**

Incorporation of  $^{15}\text{N}$ -labeled ammonium has been previously used as a proxy for protein synthesis in microbial populations at the community and cell-specific levels (Kruger et al., 2008; Orphan et al., 2009). In order to determine if aggregates that persisted in the presence of a sulfate reduction inhibitor were growing, we performed FISH-NanoSIMS analyses on five such aggregates incubated with 25 mM sodium molybdate and 2 mM  $^{15}\text{N}$ -labeled

ammonium for 7 months. Three of the aggregates from the inhibited incubation were ANME-only and had similar  $^{15}\text{N}$  incorporation values (0.56, 0.49 and 0.45 atom %; Table 1). We also examined, from the same incubation, two ANME/bacteria aggregates, one with approximately 1.3 ANME cells for every bacterial cell (0.43  $^{15}\text{N}$  atom %) and another with approximately 20 ANME cells for each bacterial cell (0.96  $^{15}\text{N}$  atom %). While these incorporation values are above that of natural abundance (0.36 atom %), all but one are below the background value determined for potential abiotic adsorption of  $^{15}\text{N}$ -ammonium (0.60 atom %; Orphan et al., 2009), suggesting no growth had occurred. These data do not rule out the possibility that the aggregates are still carrying out unknown dissimilatory reactions.

Interestingly, the one aggregate that did show significant levels of  $^{15}\text{N}$  incorporation had a unique pattern of incorporation consisting of small hot spots of  $^{15}\text{N}$  (Figure 3). While ANME/SRB aggregates typically have an ANME:SRB cell ratio of 1:2 or 1:3 (Orphan et al., 2009; Nauhaus et al., 2007), this aggregate had a much higher ANME:bacteria ratio of 20:1. Non-SRB bacteria have been reported previously in association with ANME (Pernthaler et al., 2008) and as the bacterial probe used in our study was a general one, it is possible the bacteria in this unusual configuration were not SRB, explaining the potential growth under sulfate reduction-inhibiting conditions.

A baseline level of  $^{15}\text{N}$  incorporation was also determined via measurement of aggregates incubated with 2 mM  $^{15}\text{N}$ -labeled ammonium in the absence of any inhibitors. The ANME/bacteria and ANME-only aggregates showed very similar  $^{15}\text{N}$  incorporation levels after 7 months (5.4 and 5.9 atom %, respectively; Table 1). While these levels are lower (about an order of magnitude) than what has been previously published from studies of

similar AOM microcosms (Dekas et al., 2009; Orphan et al., 2009), they are still much higher than natural abundance (0.36 atom %) as well as the background value for potential abiotic adsorption of  $^{15}\text{N}$ -ammonium (0.60 atom %; Orphan et al., 2009), confirming growth in the control incubation. Between the 1 and 7 month time points we observed a decrease in sulfide production which could indicate sulfate reduction was not occurring and therefore growth (and  $^{15}\text{N}$  incorporation) would be limited. This decrease in sulfide could also be explained by the likely presence of sulfide-oxidizing bacteria in the incubations (as discussed above). If sulfide-oxidizing bacteria were active, this could lead to the production of ammonium (seen to accumulate in Blank incubations), which would dilute the  $^{15}\text{N}$ -ammonium incorporation signal.

## CONCLUSIONS

Anaerobic methane oxidation, serving as a sink for this potent greenhouse gas, is a crucial biogeochemical process and yet little is known about the dynamics that exist between the two partners which effect this process. Numerous studies have focused on the effects of sulfate reduction inhibitors on the AOM process as a whole (Alperin and Reeburgh, 1985; Hansen et al., 1998; Iversen et al., 1987; Nauhaus et al., 2005; Orcutt et al., 2008), but the effect of these inhibitors on the cells comprising the ANME/SRB consortia remained unknown. In order to study dynamics of AOM we inhibited sulfate reduction and followed the metabolic processes of the microcosm community as well as the effect of aggregate composition and growth on a cellular level. Here we show that while bacterial cells appear to decay, ANME-2 cells persist in the form of ANME-only aggregates, which are capable of little to no growth when sulfate reduction is inhibited.

ANME-1, -2 and -3 cells have been found without a bacterial partner (Knittel and Boetius, 2009; Orphan et al., 2002; Omoregie et al., 2008), suggesting an alternative metabolism may be possible for these archaea. Our data suggest the growth and metabolism of ANME-2 is tightly linked to the bacterial partner. A study by Nauhaus et al., (2005), showed the addition of molybdate completely inhibited AOM in ANME-2 but not ANME-1 dominated communities, suggesting growth independent of sulfate reduction may have occurred. Further studies on the effects sulfate reduction-inhibition on the growth ANME-1 may reveal alternative growth requirements for ANME-1 and -2.

## ACKNOWLEDGEMENTS

We would like to acknowledge Ankur Saxena for figure design, Yunbin Guan for his assistance with NanoSIMS, and the science party of cruise AT 15-68 and pilots of the D.S.R.V. Alvin for their assistance with various aspects of this work. Funding for this work was provided by the Department of Energy Division of Biological Research (DE-SC0004949; to V.J.O.), and a National Science Foundation Graduate Research Fellowship (to A.G.-S.). Samples were collected with funding from the National Science Foundation (BIO-OCE #0825791; to V.J.O.).

## REFERENCES

- Alperin MJ & Reeburgh WS (1985) Inhibition experiments on anaerobic methane oxidation. *Applied and Environmental Microbiology* 50: 940-945.
- Amann RI, Ludwig W & Schleifer K-H (1995) Phylogenetic identification and *in situ* detection of individual microbial cells without cultivation. *Microbiological reviews* 59: 143-169.
- Boetius A, Ravenschlag K, Schubert CJ, et al. (2000) A marine microbial consortium apparently mediating anaerobic oxidation of methane. *Nature* 407: 623-626.

- Boetius A, Ravenschlag K, Schubert CJ, et al. (2000) A marine microbial consortium apparently mediating anaerobic oxidation of methane. *Nature* 407: 623-626.
- Boetius A & Suess E (2004) Hydrate Ridge: a natural laboratory for the study of microbial life fueled by methane from near-surface gas hydrates. *Chemical Geology* 205: 291-310.
- Cline JD (1969) Spectrophotometric determination of hydrogen sulfide in natural waters. *Limnology and Oceanography* 454-458.
- Compeau G & Bartha R (1985) Sulfate-reducing bacteria: principal methylators of mercury in anoxic estuarine sediment. *Applied and Environmental Microbiology* 50: 498-502.
- Dekas AD, Poretsky RS & Orphan VJ (2009) Deep-sea archaea fix and share nitrogen in methane-consuming microbial consortia. *Science* 326: 422-426.
- Dekas AE & Orphan VJ (2011) Identification of diazotrophic microorganisms in marine sediment via fluorescence *in situ* hybridization coupled to nanoscale secondary ion mass spectrometry (FISH-NanoSIMS). *Methods Enzymol* 486: 281-305.
- Hansen LB, Finster K, Fossing H & Iversen N (1998) Anaerobic methane oxidation in sulfate depleted sediments: effects of sulfate and molybdate additions. *Aquatic Microbial Ecology* 14: 195-204.
- Hoehler TM, Alperin MJ, Albert DB & Martens CS (1994) Field and laboratory studies of methane oxidation in an anoxic marine sediment: Evidence for a methanogen, sulfate reducer consortium. *Global Biogeochemical Cycles* 8: 451-463.
- Iversen N & Jørgensen B (1985) Anaerobic methane oxidation rates at the sulfate-methane transition in marine sediments from Kattegat and Skagerrak (Denmark). *Limnol. Oceanogr* 30: 944-955.
- Iversen N, Oremland RS & Klug MJ (1987) Big Soda Lake (Nevada). 3. Pelagic methanogenesis and anaerobic methane oxidation. *Limnol. Oceanogr* 32: 804-808.
- Knittel K & Boetius A (2009) Anaerobic Oxidation of Methane: Progress with an unknown process. *Annu. Rev. Microbiol.* 63: 311-334.
- Krüger M, Wolters H, Gehre M, Joye SB & Richnow HÄ (2008) Tracing the slow growth of anaerobic methane-oxidizing communities by  $^{15}\text{N}$ -labelling techniques. *FEMS microbiology ecology* 63: 401-411.
- Lovley DR, Dwyer DF & Klug MJ (1982) Kinetic analysis of competition between sulfate reducers and methanogens for hydrogen in sediments. *Applied and Environmental Microbiology* 43: 1373-1379.

Milucka J, Ferdelman TG, Polerecky L, et al. (2012) Zero-valent sulphur is a key intermediate in marine methane oxidation. *Nature* 491: 541-546.

Nauhaus K, Albrecht M, Elvert M, Boetius A & Widdel F (2007) In vitro cell growth of marine archaeal-bacterial consortia during anaerobic oxidation of methane with sulfate. *Environmental Microbiology* 9: 187-196.

Nauhaus K, Albrecht M, Elvert M, Boetius A & Widdel F (2007) In vitro cell growth of marine archaeal-bacterial consortia during anaerobic oxidation of methane with sulfate. *Environmental Microbiology* 9: 187-196.

Nauhaus K, Treude T, Boetius A & Krüger M (2005) Environmental regulation of the anaerobic oxidation of methane: a comparison of ANME-I and ANME-II communities. *Environmental Microbiology* 7: 98-106.

Omeregge EO, Mastalerz V, de Lange G, et al. (2008) Biogeochemistry and community composition of iron-and sulfur-precipitating microbial mats at the Chefren Mud Volcano (Nile Deep Sea Fan, Eastern Mediterranean). *Applied and Environmental Microbiology* 74: 3198-3215.

Orcutt B, Samarkin V, Boetius A & Joye S (2008) On the relationship between methane production and oxidation by anaerobic methanotrophic communities from cold seeps of the Gulf of Mexico. *Environmental Microbiology* 10: 1108-1117.

Orphan VJ, House CH, Hinrichs K-U, McKeegan KD & DeLong EF (2002) Multiple archaeal groups mediate methane oxidation in anoxic cold seep sediments. *Proceedings of the National Academy of Sciences* 99: 7663-7668.

Orphan VJ, House CH, Hinrichs KU, McKeegan KD & DeLong EF (2001) Methane-consuming archaea revealed by directly coupled isotopic and phylogenetic analysis. *Science* 293: 484-487.

Orphan VJ, Turk KA, Green AM & House CH (2009) Patterns of <sup>15</sup>N assimilation and growth of methanotrophic ANME-2 archaea and sulfate-reducing bacteria within structured syntrophic consortia revealed by FISH-SIMS. *Environ Microbiol* doi:10.1111/ j.1462-2920.2009.01903.x.

Pernthaler A, Dekas AE, Brown CT, Goffredi SK, Embaye T & Orphan VJ (2008) Diverse syntrophic partnerships from deep-sea methane vents revealed by direct cell capture and metagenomics. *Proc Natl Acad Sci U S A* 105: 7052-7057.

Preisler A, de Beer D, Lichtschlag A, Lavik G, Boetius A & Jorgensen BB (2007) Biological and chemical sulfide oxidation in a Beggiatoa inhabited marine sediment. *ISME J* 1: 341-353.

Reeburgh WS (1976) Methane consumption in Cariaco Trench waters and sediments. *Earth and Planetary Science Letters* 28: 337-344.

Reeburgh WS (2007) Oceanic methane biogeochemistry. *Chemical Reviews* 107: 486-513.

Reuveny Z (1977) Derepression of ATP sulfurylase by the sulfate analogs molybdate and selenate in cultured tobacco cells. *Proceedings of the National Academy of Sciences* 74: 619-622.

Schiermeier Q (2006) Methane finding baffles scientists. *Nature* 439: 128-128.

## **FIGURES and TABLES**

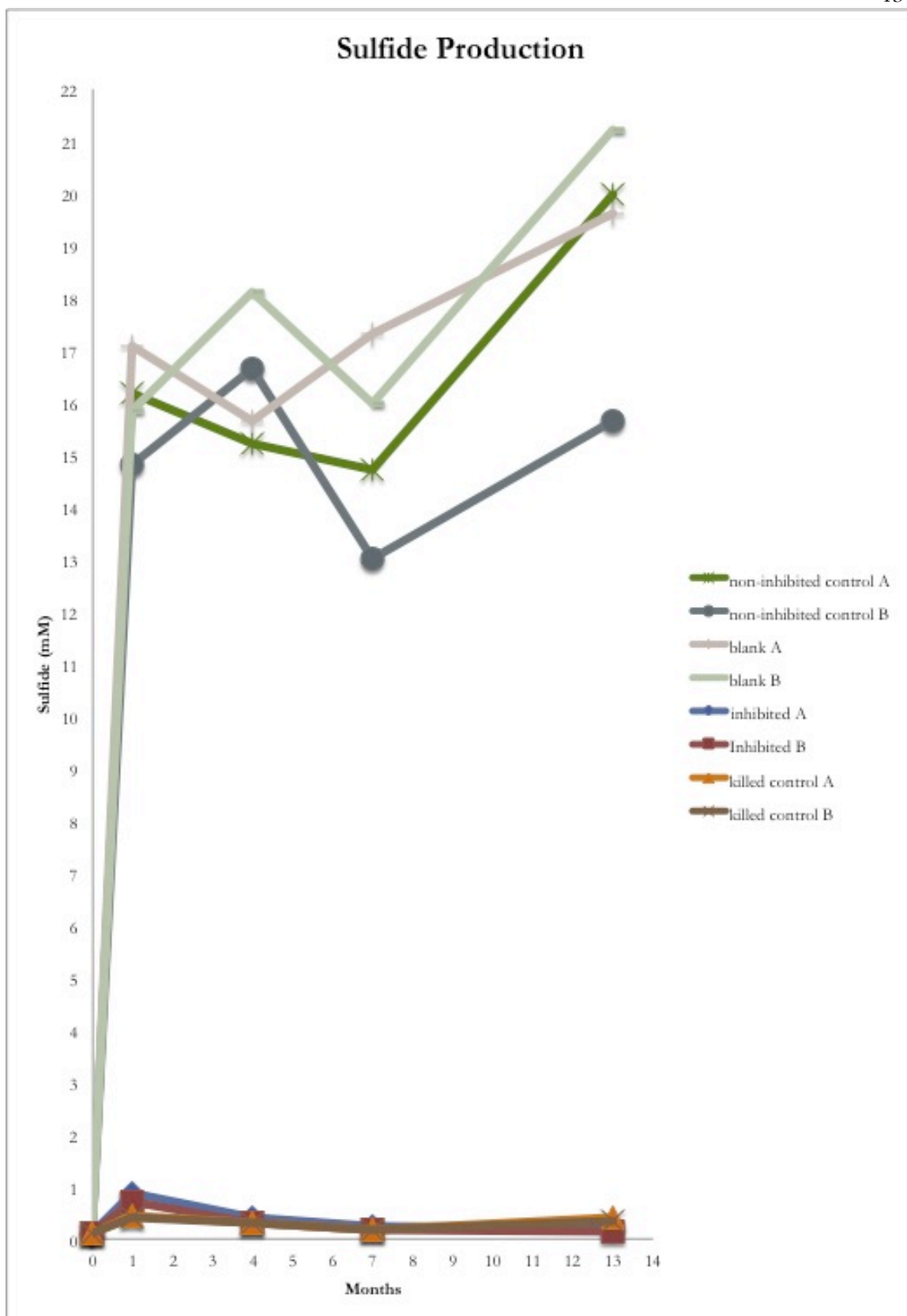


**Figure 1a.**

Sulfide production measured in 4 duplicate sets of incubations over 13 months. Control incubations were amended with 2 mM  $^{15}\text{N}$ -ammonium; blank incubations had no amendments; inhibited incubations were amended with 2 mM  $^{15}\text{N}$ -ammonium and 25 mM sodium molybdate; killed controls were amended with 2 mM  $^{15}\text{N}$ -ammonium and treated with 3.7 % formaldehyde at the initial time point.

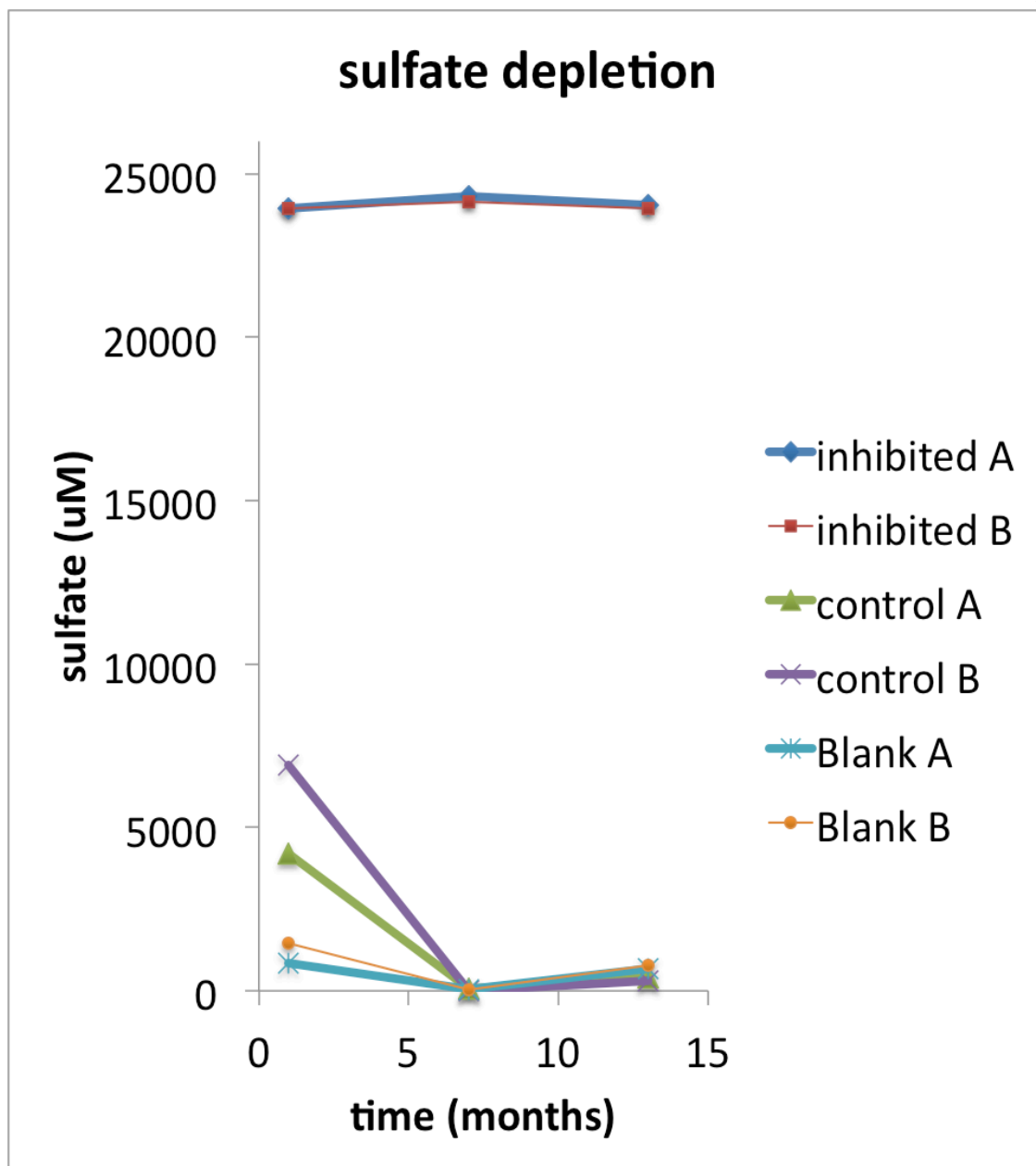


**Figure 1b.**

Sulfate depletion measured in 3 duplicate sets of incubations over 13 months. Control incubations were amended with 2 mM  $^{15}\text{N}$ -ammonium; blank incubations had no amendments; inhibited incubations were amended with 2 mM  $^{15}\text{N}$ -ammonium and 25 mM sodium molybdate.

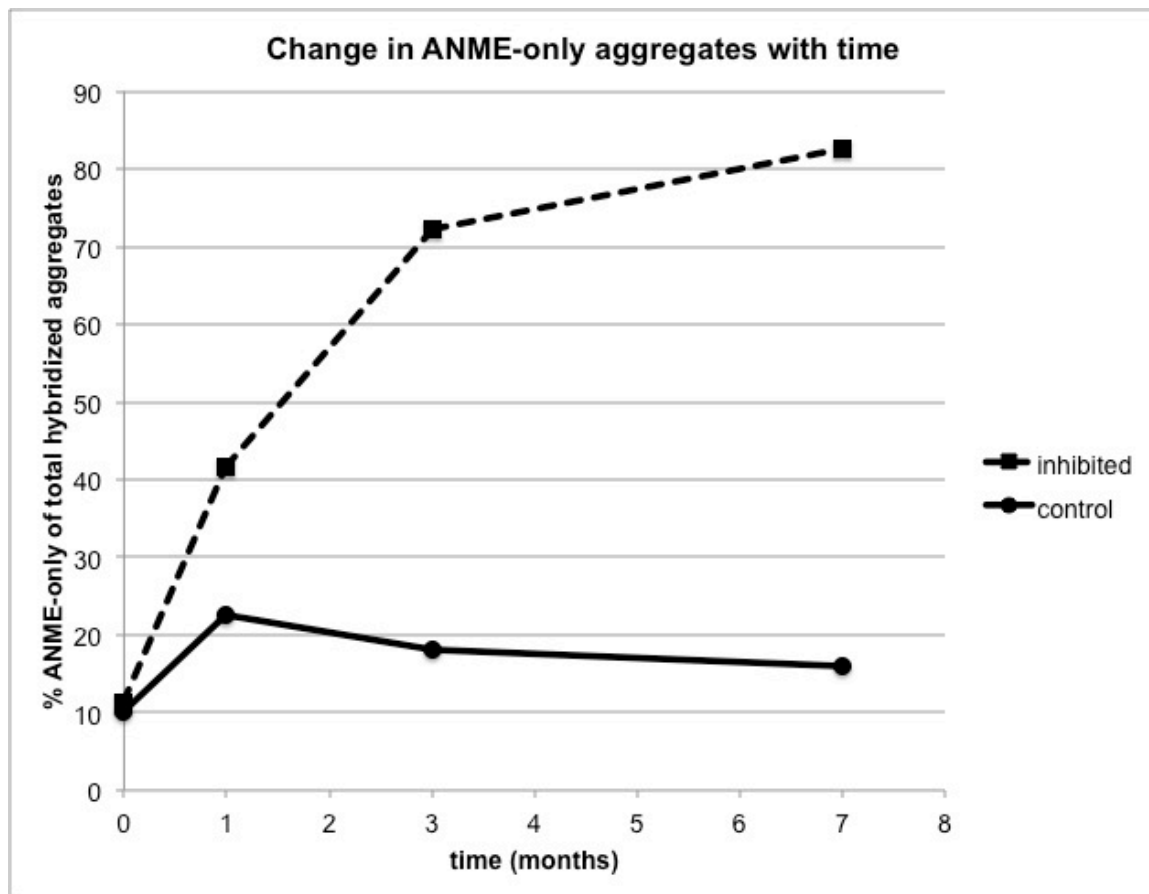


**Figure 2.**

Change in aggregate composition over time. ANME/bacteria and ANME-only aggregates were counted from samples taken at 0, 1, 4 and 7 months. Cy3- and FITC-labeled oligonucleotide probes Eel\_MS\_932 (ANME-2; Boetius et al., 2000) and EUB338 (general bacteria; Amann et al., 1995), respectively, were used in FISH reactions. Aggregates counts are expressed as the percent of ANME-only aggregates out of all ANME-only and ANME/bacteria aggregates counted (each point represents 50 aggregates-containing fields counted).

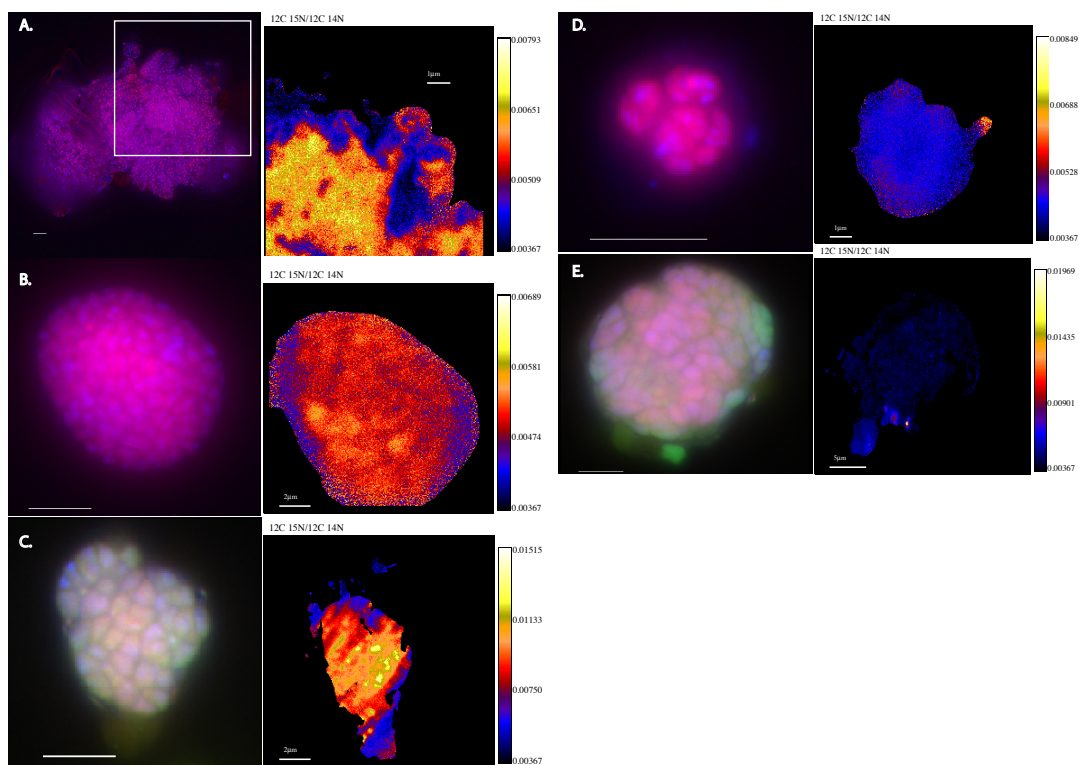


**Figure 3.**

Corresponding FISH and ion micrographs of aggregates examined via FISH-NanoSIMS from the inhibited incubation, amended with 2 mM  $^{15}\text{N}$ -ammonium and 25 mM sodium molybdate and sampled at 7 months. Cy3- and FITC-labeled oligonucleotide probes Eel\_MS\_932 (ANME-2; Boetius et al., 2000) and EUB338 (general bacteria; Amann et al., 1995), respectively, were used in FISH reactions. FISH micrograph lettering corresponds to aggregate name in Table 1. Scale bars in FISH micrographs represent 5  $\mu\text{m}$ .

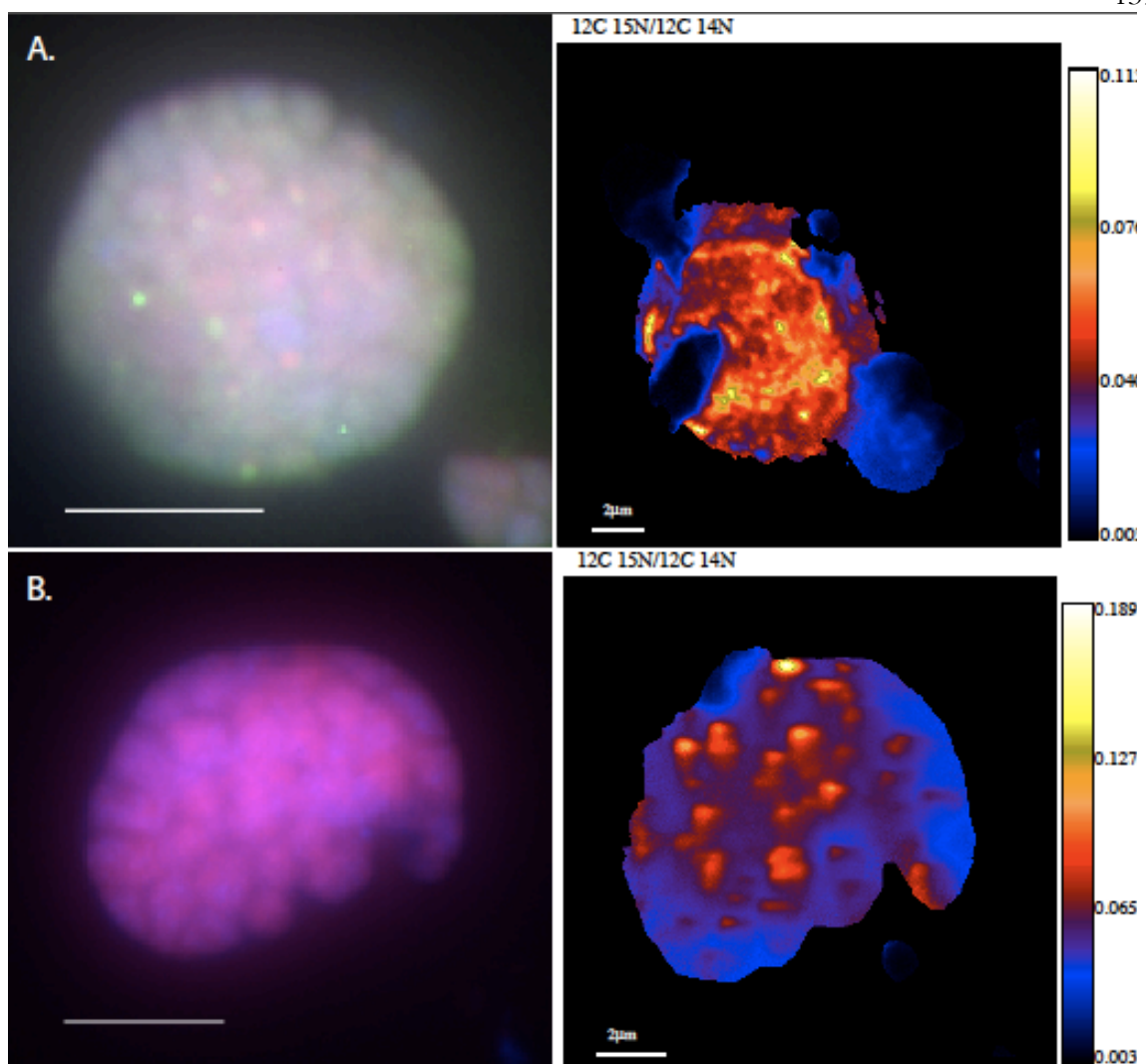


**Figure 4.**

Corresponding FISH and ion micrographs of aggregates examined via FISH-NanoSIMS from the control incubation (no inhibitor), amended with 2 mM  $^{15}\text{N}$ -ammonium and sampled at 7 months. Cy3- and FITC-labeled oligonucleotide probes Eel\_MS\_932 (ANME-2; Boetius et al., 2000) and EUB338 (general bacteria; Amann et al., 1995), respectively, were used in FISH reactions. FISH micrograph lettering corresponds to aggregate name in Table 1. Scale bars in FISH micrographs represent 5  $\mu\text{m}$ .

Table 1.  $^{15}\text{N}$  atom % (highest cycle avg.) of each aggregate investigated via NanoSIMS.

<b>incubation</b>	<b>aggregate</b>	<b><math>^{15}\text{N}</math> atom % (highest cycle avg.)</b>
inhibited	A (ANME only)	0.5570
inhibited	B (ANME only)	0.4940
inhibited	C (ANME/bacteria)	0.9560
inhibited	D (ANME only)	0.4540
inhibited	E (ANME/bacteria)	0.4290
control	A (ANME/bacteria)	5.3720
control	B (ANME only)	5.9140